# Two-mode lasing without inversion with injected atomic coherence

Pál Bogár and János A. Bergou

*Department of Physics and Astronomy, Hunter College of the City University of New York,*
*695 Park Avenue, New York, New York 10021*

Noninversion lasing is investigated in $\Lambda$-type three-level atomic systems that are coupled to two modes of the electromagnetic field. As a result of an external field driving the transition between the lower two closely spaced levels, laser action can be achieved in both modes simultaneously at arbitrarily small initial upper-level population (lasing without inversion) provided the pumping rate exceeds a certain threshold. The relative phase of the two modes is locked to a particular value controlled by the phase of the external field. In addition, new regimes of the laser operation arise when initial coherences between various atomic levels are also injected into the resonator. Firstly, laser action can be achieved in both modes at arbitrarily small pumping (no threshold). Secondly, the injected atomic coherence can control competition between the modes, and result in a variety of multistable steady-state behavior illustrating the very sensitive dynamics of the system. [S1050-2947(97)09807-7]

## I. INTRODUCTION

In recent years, a considerable amount of theoretical and experimental research has been devoted to atomic coherence effects in laser systems. The motivation behind this work is both fundamental and applied physics. It targets the microscopic mechanism of the emission of light employing active atoms in coherent superpositions of their quantum states involved in the laser action and, on the other hand, searches for practical applications of these mechanisms in constructing new types of lasers and other quantum optical devices. The signature of driving atomic coherence can be traced in the performance of the laser, viz., in the dynamical and noise characteristics of the radiation. It has been demonstrated, to consider a prominent example, that atomic coherence established between two closely spaced lower levels of three-level ($\Lambda$-type) atoms using an external field [1] may lead to laser action even though the active medium is not in an inverted state [lasing without inversion (LWI) [1–3]]. One interpretation of this effect is that atomic coherence results in nonabsorbing resonances in the system [4]. In addition, injecting initial atomic coherence between all three levels of the driving atoms can lead to an elimination of the pumping threshold for laser operation, another long-thought key concept of the conventional laser theories, and the system enters its nonlinear regime at arbitrarily small pumping [5]. This is the consequence of the injected atomic coherence, i.e., a driving atomic dipole, that radiates independently of the actual incoherent gain-loss ratio in the system. Furthermore, injected atomic coherence can also result in a simultaneous reduction of photon-number noise and phase noise in the laser [5]. The possibility to significantly reduce the noise in laser systems and produce, for example, squeezed light using injected atomic coherence has attracted much attention in the past few years [6,7]. The practical applications of these quantum coherence phenomena in active optical systems are obvious. Noninversion lasing could be very useful in, for example, regimes where inversion is difficult to establish, due to high rate of spontaneous emission (i.e., in the high-frequency, vacuum ultraviolet, or x-ray, domain of the spectrum), while reduced-noise radiation could be advantageous in, for example, optical communication networks. Let us also mention here two other prominent quantum optical concepts related to effects of atomic coherence. These are the enhanced index of refraction with minimal absorption as suggested by Scully and collaborators [8], and the electromagnetically induced transparency demonstrated by Harris and co-workers [9]. We also note the recently proposed method of generating atomic coherence utilizing a Stark-shifted sublevel crossing a neighboring atomic state by Kocharovskaya *et al.* [10].

Motivated by the above examples illustrating the significance of atomic coherence in quantum optical systems we consider here a two-mode version of the above-mentioned $\Lambda$-type three-level LWI systems [5]. The transition between the lower two closely spaced levels is driven by an external field and, in addition, atomic coherences between various states of the three-level atoms are injected. The competition between the modes is investigated, together with the onset of noninversion lasing and zero-threshold operation in both modes. We find that atomic coherences play a crucial role in the competition between the two modes; they can be applied, in some cases, to redistribute the energy between the two modes while, in others, they result in instabilities and multistable steady-state behavior of the laser modes. These instabilities and the very sensitive dynamics exhibiting critical behavior in the two-mode system suggest that selection of a single mode in the experimental realization of LWI can be an essential condition in achieving stable operation.

In the next section we present the model of the system by introducing its Hamiltonian and transforming it into an interaction picture. The resulting Schrödinger equation is solved in Sec. III for the time-dependent wave function that, in Sec. IV, is used to derive the master equation for the field-density matrix. In Sec. V we transform the master equation into a Fokker-Planck equation for the $P$ function. The drift coefficients of the equation are then analyzed in Sec. VI to de-
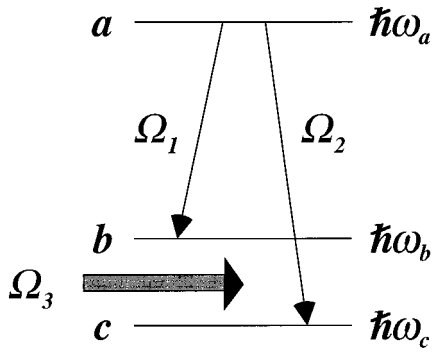
FIG. 1. Scheme of a two-mode laser driven by $\Lambda$-type three-level atoms where the two laser modes of frequencies $\Omega_1$ and $\Omega_2$ couple the upper level $a$ to the lower two levels $b$ and $c$ and the external field $\Omega_3$ drives the transition between the lower two closely spaced levels $b$ and $c$.

scribe the dynamical behavior of the average intensities and phases of the two modes considering various schemes for injected atomic coherences. Finally, we conclude in Sec. VII.

## II. THE MODEL

We consider a system of $\Lambda$-type three-level atoms, as shown in Fig. 1, where the $|a\rangle \rightarrow |b\rangle$ and $|a\rangle \rightarrow |c\rangle$ transitions are coupled to two cavity modes of frequencies $\Omega_1$ and $\Omega_2$, respectively. The two closely spaced lower levels, $|b\rangle$ and $|c\rangle$, are strongly driven by an external (classical) field characterized by the Rabi frequency $\mathcal{V}$, frequency $\Omega_3$, and phase $\phi$. We also assume injected coherence between the atomic states, i.e., the corresponding off-diagonal elements of the initial atomic density matrix are different from zero. This is almost the same system as the one studied in Ref. [5]

in detail, except here we allow for two separate modes contributing to (competing for) the laser action. Since the formulation and solution closely parallels Ref. [5] we confine ourselves to a brief outline of the model and its solution.

The Hamiltonian for the field and one active atom in the Schrödinger picture is given by

$$H = H_0 + V, \tag{2.1}$$

where

$$H_0 = \sum_{i=a,b,c} \hbar \omega_i |i\rangle\langle i| + \hbar\Omega_1(a_1^\dagger a_1 + 1/2) + \hbar\Omega_2(a_2^\dagger a_2 + 1/2) \tag{2.2}$$

and

$$V = \hbar g_1 a_1 |a\rangle\langle b| + \hbar g_2 a_2 |a\rangle\langle c|$$
$$- \tfrac{1}{2}\hbar\mathcal{V}e^{-i(\Omega_3 t + \phi)}|b\rangle\langle c| + \text{H.c.} \tag{2.3}$$

Here $a_1$ ($a_1^\dagger$) and $a_2$ ($a_2^\dagger$) are the annihilation (creation) operators for the two cavity modes, $g_1$ and $g_2$ are the coupling constants for the $|a\rangle \rightarrow |b\rangle$ and $|a\rangle \rightarrow |c\rangle$ transitions, respectively. The external microwave field is treated semiclassically. Let us define the first interaction picture as

$$V_I = e^{(i/\hbar)H_0 t} V e^{-(i/\hbar)H_0 t}. \tag{2.4}$$

After breaking $V_I$ up into two terms as $V_I = V_1 + V_2$, where

$$V_1 = -\frac{1}{2}\hbar\mathcal{V}\begin{bmatrix} 0 & 0 & 0 \\ 0 & 0 & \exp(i\Delta_3 t - i\phi) \\ 0 & \exp(-i\Delta_3 t + i\phi) & 0 \end{bmatrix} \tag{2.5}$$

and

$$V_2 = \hbar\begin{bmatrix} 0 & g_1 a_1 \exp(i\Delta_1 t) & g_2 a_2 \exp(i\Delta_2 t) \\ g_1 a_1^\dagger \exp(-i\Delta_1 t) & 0 & 0 \\ g_2 a_2^\dagger \exp(-i\Delta_2 t) & 0 & 0 \end{bmatrix}, \tag{2.6}$$

we use $V_1$ and $V_2$ to define the second interaction picture

$$V_{II} = e^{(i/\hbar)V_1 t} V_2 e^{-(i/\hbar)V_1 t}. \tag{2.7}$$

The detunings above are defined as $\Delta_1 = \omega_{ab} - \Omega_1$, $\Delta_2 = \omega_{ac} - \Omega_2$, and $\Delta_3 = \omega_{bc} - \Omega_3$, where $\omega_{ij} = \omega_i - \omega_j$, $i,j = a,b,c$. We assume that the classical driving field is resonant, $\Delta_3 = 0$, and the fields in the two laser modes are detuned as $\Delta_1 = -\Delta_2 = \mathcal{V}/2 \gg \gamma$. Here $\gamma$ is the atomic decay rate (common to all levels) as introduced in the next section. Then, applying the rotating-wave approximation by neglecting the rapidly varying exponentials (and retaining the slowly varying ones), lower signs in $\exp[i(\Delta_1 \pm \mathcal{V}/2)t]$ and upper signs in $\exp[i(\Delta_2 \pm \mathcal{V}/2)t]$, we arrive at the interaction matrix

$$V_{II} = \frac{1}{2}\hbar g\begin{bmatrix} 0 & a_1 - e^{i\phi}a_2 & a_2 + e^{-i\phi}a_1 \\ a_1^\dagger - e^{-i\phi}a_2^\dagger & 0 & 0 \\ a_2^\dagger + e^{i\phi}a_1^\dagger & 0 & 0 \end{bmatrix}, \tag{2.8}$$

provided $g \equiv g_1 = g_2$. The corresponding result for the single-mode system in Ref. [5] is reobtained when $a_1 = a_2$ is assumed.

## III. SOLUTION OF THE MODEL

Using the interaction Hamiltonian given by Eq. (2.8) we find the time evolution of the wave function of the $\Lambda$ system by solving the time-dependent Schrödinger equation in the second interaction picture,

$$i\hbar\,\dot{\psi}=V_{II}\psi. \tag{3.1}$$

Here, $\psi$ is a column vector of the three components, $\psi_a, \psi_b, \psi_c$, and Eq. (3.1) is a system of three coupled differential equations for the three components that read as

$$i\dot{\psi}_a=\frac{1}{2}\,g(a_1-e^{i\phi}a_2)\psi_b+\frac{1}{2}\,g(a_2+e^{-i\phi}a_1)\psi_c-i\,\frac{\gamma}{2}\,\psi_a, \tag{3.2}$$

$$i\dot{\psi}_b=\frac{1}{2}\,g(a_1^\dagger-e^{-i\phi}a_2^\dagger)\psi_a-i\,\frac{\gamma}{2}\,\psi_b, \tag{3.3}$$

$$i\dot{\psi}_c=\frac{1}{2}\,g(a_2^\dagger+e^{i\phi}a_1^\dagger)\psi_a-i\,\frac{\gamma}{2}\,\psi_c. \tag{3.4}$$

The atomic relaxation is introduced via the last terms on the right-hand sides, where $\gamma$ is the decay constant for the three atomic levels $a,b,c$, for simplicity, assumed to be the same for all levels. Similarly to Ref. [5], this system can be solved simultaneously by introducing the new functions, $\widetilde{\psi}_a$, $\widetilde{\psi}_+$, and $\widetilde{\psi}_-$, defined by

$$\psi_a=e^{-\gamma/2(t-t_0)}\widetilde{\psi}_a, \tag{3.5}$$

$$\psi_b=e^{-\gamma/2(t-t_0)}e^{-i\phi/2}(B_-^\dagger\widetilde{\psi}_++B_+\widetilde{\psi}_-), \tag{3.6}$$

$$\psi_c=e^{-\gamma/2(t-t_0)}e^{i\phi/2}(B_+^\dagger\widetilde{\psi}_+-B_-\widetilde{\psi}_-), \tag{3.7}$$

where

$$B_+=\tfrac{1}{2}(a_1e^{-i\phi/2}+a_2e^{i\phi/2}), \tag{3.8}$$

$$B_-=\tfrac{1}{2}(a_1e^{-i\phi/2}-a_2e^{i\phi/2}). \tag{3.9}$$

In this way, the three differential equations given by Eqs. (3.2)–(3.4) become

$$\dot{\widetilde{\psi}}_a=-igA\widetilde{\psi}_+, \tag{3.10}$$

$$\dot{\widetilde{\psi}}_+=-ig\widetilde{\psi}_a, \tag{3.11}$$

$$\dot{\widetilde{\psi}}_-=0, \tag{3.12}$$

where

$$A=\tfrac{1}{2}(a_1a_1^\dagger+a_2a_2^\dagger), \tag{3.13}$$

and their simultaneous solutions are given by

$$\widetilde{\psi}_a(t)=C\widetilde{\psi}_a(t_0)-iAS\widetilde{\psi}_+(t_0), \tag{3.14}$$

$$\widetilde{\psi}_+(t)=C\widetilde{\psi}_+(t_0)-iS\widetilde{\psi}_a(t_0), \tag{3.15}$$

$$\widetilde{\psi}_-(t)=\widetilde{\psi}_-(t_0), \tag{3.16}$$

where $C=\cos[g(t-t_0)A^{1/2}]$ and $S=A^{-1/2}\sin[g(t-t_0)A^{1/2}]$. The solutions for $\psi_a, \psi_b, \psi_c$ can be obtained from Eqs. (3.14)–(3.16) using the definitions, Eqs. (3.5)–(3.7), in a straightforward way. We shall use these solutions in the next section to find the master equation for the field-density operator.

## IV. THE MASTER EQUATION

The density operator of the three-level $\Lambda$ atom and the two-mode field satisfies the following equation of motion in the second interaction picture:

$$\dot{\rho}=-\frac{i}{\hbar}\,[V_{II},\rho]. \tag{4.1}$$

We want to study the behavior of the field only. To obtain the reduced density operator for the field, $\rho_F$, we trace the atom-field density operator over the atomic variables, $\rho_F=\mathrm{Tr}_{\mathrm{atom}}\rho$. Thus, the equation of motion for $\rho_F$ is obtained from Eq. (4.1) as

$$\dot{\rho}_F=\mathrm{Tr}_{\mathrm{atom}}\dot{\rho}=-\frac{i}{\hbar}\,\mathrm{Tr}_{\mathrm{atom}}[V_{II},\rho]. \tag{4.2}$$

Using the interaction matrix, $V_{II}$, given by Eq. (2.8), Eq. (4.2) reads

$$\dot{\rho}_F=-ig\{e^{-i\phi/2}([B_-^\dagger,\bar{\rho}_{ab}]+[B_+,\bar{\rho}_{ca}])+e^{i\phi/2}([B_-,\bar{\rho}_{ba}]$$
$$+[B_+^\dagger,\bar{\rho}_{ac}])\}+L_1\rho_F+L_2\rho_F. \tag{4.3}$$

Here, $\mathcal{L}_i\rho_F$, $i=1,2$, accounts for the effect of field losses in the two modes due to cavity damping, and it is explicitly given by

$$\mathcal{L}_i\rho_F=-\frac{\gamma_c}{2}\,(a_i^\dagger a_i\rho_F+\rho_Fa_i^\dagger a_i-2a_i\rho_Fa_i^\dagger), \tag{4.4}$$

where $\gamma_c$ is the cavity damping rate, assumed to be the same for both modes. Here $\bar{\rho}_{ab}$ and $\bar{\rho}_{ac}$ stand for the matrix elements of the total atom-field density operator. To obtain their explicit expressions we first calculate the contribution of one atom injected at time $t_0$ with arbitrary initial condition into the cavity and then sum the contributions of all atoms injected at random times between $t-1/\gamma$ and $t$ (i.e., $t-1/\gamma<t_0<t$) at rate $r$. This means that the atom-field interaction is considered on a time scale shorter than the atomic lifetime $1/\gamma$. In this way,

$$\bar{\rho}_{ab}=r\int_{t-1/\gamma}^t dt_0\,\psi_a(t,t_0)\psi_b^\dagger(t,t_0) \tag{4.5}$$

and

$$\bar{\rho}_{ac}=r\int_{t-1/\gamma}^t dt_0\,\psi_a(t,t_0)\psi_c^\dagger(t,t_0). \tag{4.6}$$

Substituting the solutions obtained for $\psi_a, \psi_b, \psi_c$ in the previous section into Eqs. (4.5) and (4.6) we calculate the matrix elements as follows. Since the dynamics of the field is governed by the cavity lifetime $1/\gamma_c$, which is much longer then the atomic lifetime, $1/\gamma$, $\rho_F$ does not change appreciably during the integration time interval, and thus $\rho_F(t_0)$ in Eqs. (4.5) and (4.6) can be approximated by $\rho_F(t)$. On the other hand, when $t-t_0>1/\gamma$ (i.e., $t-1/\gamma>t_0$) the contribution to the integral is negligible due to the exponential damping factor. This means that the lower limit of the integration can be extended to $-\infty$. After performing these steps and carrying out the integral we can substitute the results for

$\bar{\rho}_{ab}$, $\bar{\rho}_{ac}$ and their Hermitian conjugates into the equation of motion in Eq. (4.3) and obtain the final form of the master equation for the field-density matrix.

We want to remark here that when we took the trace over the atomic variables in Eq. (4.2) then, in the matrix elements appearing on the right-hand side in Eq. (4.3) and calculated according to Eqs. (4.5) and (4.6), we effectively replaced the atomic variables by their steady-state values (adiabatic elimination of atomic variables). This is justified by the much faster atomic relaxation rate than that of the field ($\gamma \gg \gamma_c$). In doing so, we made use of our solution for the wave function in Eqs. (3.14)–(3.16) and, therefore, in the resulting master equation the atomic relaxation process is fully accounted for.

The explicit but rather complicated form of the master equation will not be given here. Instead, in the next section, we transform it into a Fokker-Planck equation and, analyzing the drift coefficients of the equation, we study the dynamics of the two-mode field.

## V. THE FOKKER-PLANCK EQUATION

### A. Derivation of the Fokker-Planck equation

In this section we employ the Glauber-Sudarshan $P$ representation for the field-density matrix to transform the operator master equation given implicitly by Eq. (4.3) into a $c$-number differential equation, the Fokker-Planck equation, for the $P$ function. An outline of the standard procedure is given in the Appendix; here we present the final results only. Using the normalized intensities, $\widetilde{I}_i = (\beta/\alpha)I_i$, where $\alpha \equiv (r/\gamma_c)g^2/\gamma^2$ and $\beta \equiv 4(r/\gamma_c)g^4/\gamma^4$ are the respective pumping and saturation parameters, and the phases $\theta_i$ of the two field modes, $i = 1,2$, as the variables of the $P$ function, $P = P(\widetilde{I}_1, \widetilde{I}_2, \theta_1, \theta_2, t)$, we arrive at the Fokker-Planck equation given by

$$\frac{1}{\gamma_c}\frac{\partial P}{\partial t} = \{-\partial_{\widetilde{I}_1}d_{\widetilde{I}_1} - \partial_{\theta_1}d_{\theta_1} + \partial^2_{\widetilde{I}_1\widetilde{I}_1}D_{\widetilde{I}_1\widetilde{I}_1} + \partial^2_{\theta_1\theta_1}D_{\theta_1\theta_1}$$
$$+ \partial^2_{\widetilde{I}_1\theta_1}D_{\widetilde{I}_1\theta_1} - \partial_{\widetilde{I}_2}d_{\widetilde{I}_2} - \partial_{\theta_2}d_{\theta_2} + \partial^2_{\widetilde{I}_2\widetilde{I}_2}D_{\widetilde{I}_2\widetilde{I}_2}$$
$$+ \partial^2_{\theta_2\theta_2}D_{\theta_2\theta_2} + \partial^2_{\widetilde{I}_2\theta_2}D_{\widetilde{I}_2\theta_2} + \partial^2_{\widetilde{I}_1\widetilde{I}_2}D_{\widetilde{I}_1\widetilde{I}_2}$$
$$+ \partial^2_{\theta_1\theta_2}D_{\theta_1\theta_2} + \partial^2_{\widetilde{I}_1\theta_2}D_{\widetilde{I}_1\theta_2} + \partial^2_{\widetilde{I}_2\theta_1}D_{\widetilde{I}_2\theta_1}\}P + \cdots .$$
$$(5.1)$$

Here we used the notation $\partial_{x_i} = \partial/\partial x_i$ and $\partial^2_{x_iy_j} = \partial^2/\partial x_i\partial y_j$ for the derivatives, where $x_i$ and $y_i$ are any of the normalized intensity and phase variables of the two modes, $i = 1,2$, while the higher-order terms $\partial^3_{x_iy_jz_k}$ are omitted. The coefficients under the derivatives, the drift ($d$) and diffusion ($D$) terms of the equation can be used to analyze the system without solving the equation for the $P$ function. We introduce the notation $\rho_{ij} = \sqrt{\rho_{ii}\rho_{jj}}e^{i\varphi_{ij}}$, $i,j = a,b,c$, for the injected atomic coherences (which are different from the matrix elements $\bar{\rho}_{ab}$ and $\bar{\rho}_{ac}$ of the total atom-field density operator). It should be noted that the phases are constant; i.e., all atoms are prepared with the same initial phase relative to the field. The problem of the preparation of the phase is discussed in detail in Ref. [11]. For the case when the mean intensities

$\langle I_1 \rangle$ and $\langle I_2 \rangle$ are much larger than 1, the explicit expressions for the drift coefficients of the above equation read as

$$d_{\widetilde{I}_1} = \frac{\widetilde{I}_1}{N_1N_2}\left[\alpha\left(\rho_{aa} - \frac{1}{2}\bar{M}_1\right)N_1\right.$$
$$\left. - \frac{3}{16}\alpha\widetilde{I}_2(\bar{M}_1 - \bar{M}_2) - N_1N_2\right], \quad (5.2)$$

$$d_{\theta_1} = \frac{\alpha}{4N_1}\left[M_b - 4\frac{R_3}{\sqrt{\widetilde{I}_1}} - \frac{1}{2}\sqrt{\widetilde{I}_1\widetilde{I}_2}\left(\frac{R_3}{\sqrt{\widetilde{I}_2}} - \frac{R_4}{\sqrt{\widetilde{I}_1}}\right)\right], \quad (5.3)$$

and

$$d_{\widetilde{I}_2} = d_{\widetilde{I}_1}(\text{interchange, } \widetilde{I}_1 \Leftrightarrow \widetilde{I}_2 \text{ and } \bar{M}_1 \Leftrightarrow \bar{M}_2), \quad (5.4)$$

$$d_{\theta_2} = -d_{\theta_1}(\text{interchange, } \widetilde{I}_1 \Leftrightarrow \widetilde{I}_2 \text{ and } R_3 \Leftrightarrow R_4), \quad (5.5)$$

where

$$N_1 = 1 + \tfrac{1}{8}(\widetilde{I}_1 + \widetilde{I}_2), \quad (5.6)$$

$$N_2 = 1 + \tfrac{1}{2}(\widetilde{I}_1 + \widetilde{I}_2), \quad (5.7)$$

$$M_1 = \rho_{bb} + \rho_{cc} + 2|\rho_{bc}|\cos(\varphi_{bc} + \phi), \quad (5.8)$$

$$M_2 = \rho_{bb} + \rho_{cc} - 2|\rho_{bc}|\cos(\varphi_{bc} + \phi), \quad (5.9)$$

$$M_a = (\rho_{bb} - \rho_{cc})\cos(\phi - \theta) - 2|\rho_{bc}|\sin(\varphi_{bc} + \phi)\sin(\phi - \theta), \quad (5.10)$$

$$M_b = (\rho_{bb} - \rho_{cc})\sin(\phi - \theta) + 2|\rho_{bc}|\sin(\varphi_{bc} + \phi)\cos(\phi - \theta), \quad (5.11)$$

$$R_1 = |\rho_{ab}|\sin(\varphi_{ab} - \theta_1) + |\rho_{ac}|\sin(\varphi_{ac} + \phi - \theta_1), \quad (5.12)$$

$$R_2 = -|\rho_{ab}|\sin(\varphi_{ab} - \phi - \theta_2) + |\rho_{ac}|\sin(\varphi_{ac} - \theta_2), \quad (5.13)$$

$$R_3 = |\rho_{ab}|\cos(\varphi_{ab} - \theta_1) + |\rho_{ac}|\cos(\varphi_{ac} + \phi - \theta_1), \quad (5.14)$$

$$R_4 = |\rho_{ab}|\cos(\varphi_{ab} - \phi - \theta_2) - |\rho_{ac}|\cos(\varphi_{ac} - \theta_2), \quad (5.15)$$

$$\bar{M}_1 = M_1 - M_a\left(\frac{\widetilde{I}_2}{\widetilde{I}_1}\right)^{1/2} - \frac{4R_1}{\sqrt{\widetilde{I}_1}}, \quad (5.16)$$

$$\bar{M}_2 = M_2 - M_a\left(\frac{\widetilde{I}_1}{\widetilde{I}_2}\right)^{1/2} - \frac{4R_2}{\sqrt{\widetilde{I}_2}}. \quad (5.17)$$

Above, we have also introduced the relative phase between the two modes denoted by $\theta \equiv \theta_1 - \theta_2$. Its drift coefficient can be calculated as $d_\theta = d_{\theta_1} - d_{\theta_2}$. In order to completely determine the Fokker-Planck equation (5.1) we give the diffusion terms in the Appendix. A very similar set of equations for a $V$ system with initial coherence between closely spaced upper two levels has been derived in Ref. [12]. It has been shown to lead to spontaneous emission cancellation just like the cancellation of absorption in our $\Lambda$ system.

In the next subsection we outline the procedure employing the drift terms of the equation to investigate the dynamical behavior of the average intensities and phases of the two

fields. On the other hand, the diffusion terms prove useful in studying the noise performance of the field. We are not going to deal with these problems in the present paper but, together with the correlations building up between the two modes, they are planned to be the subject of future work.

### B. Applying the drift terms of the Fokker-Planck equation

Having the Fokker-Planck equation at hand, we now employ the drift coefficients to investigate the time-dependent and steady-state properties of the average intensities and phases of the two field modes. We should mention at this point that in the $P$ representation the (stochastic) average of the intensity is directly connected to the (quantum mechanical) expectation value of the photon number as $\langle I_i \rangle = \langle n_i \rangle$, $i=1,2$. It can be shown in general that

$$\frac{1}{\gamma_c} \frac{d}{dt} \langle x \rangle = \langle d_x \rangle, \tag{5.18}$$

where $x$ is any of the four dynamical variables of the equation: $\tilde{I}_1$, $\tilde{I}_2$, $\theta_1$, and $\theta_2$. After expanding the drift coefficients $d_x$ in terms of $\delta x = x - \langle x \rangle$ around the average, $\langle x \rangle$, Eq. (5.18) becomes

$$\frac{1}{\gamma_c} \frac{d}{dt} \langle x \rangle \cong d_x |_{\langle \text{all} \rangle}, \tag{5.19}$$

where the drift coefficient $d_x$ is taken at the average values of all the dynamical variables on the right-hand side. Solving the system of differential equations given by Eq. (5.19) we can find the time dependence of the average quantities, while the system of the algebraic equations, $d_x |_{\langle \text{all} \rangle} = 0$, yields the steady state.

We investigate the stability of the steady states by studying the stability of the phases of the two modes, $\theta_1$ and $\theta_2$ (for the sake of simplicity, we omit the stochastic average signs, $\langle \ \rangle$, from now on). In doing so, we introduce small perturbations, $\Delta \theta_1$ and $\Delta \theta_2$, around the steady state, $\theta_{1,s}$ and $\theta_{2,s}$, and substitute $\theta_1(t) = \theta_{1,s} + \Delta \theta_1$ and $\theta_2(t) = \theta_{2,s} + \Delta \theta_2$ into the corresponding form of Eq. (5.18). Expanding $d_{\theta_1}$ and $d_{\theta_2}$ around the steady state to first order in $\Delta \theta_1$ and $\Delta \theta_2$ we arrive at the system of two linear differential equations,

$$\frac{d\Delta \theta_i}{dt} = \frac{\partial d_{\theta_i}}{\partial \theta_1}\bigg|_{\langle \text{all} \rangle} \Delta \theta_1 + \frac{\partial d_{\theta_i}}{\partial \theta_2}\bigg|_{\langle \text{all} \rangle} \Delta \theta_2, \tag{5.20}$$

where $i=1,2$, and the derivatives are to be evaluated at steady state. We can assume that, since this is a system of linear equations, a simple exponential solution exists in the form $\Delta \theta_i(t) = \Delta \theta_i(0) e^{\lambda t}$. The characteristic equation after substituting this ansatz back into the above equations is a quadratic algebraic equation for $\lambda$, where the negative definiteness of the roots can be analyzed applying Hurwitz's criteria. If $\text{Re}\lambda < 0$ the initial perturbation decays exponentially back to the steady state while a positive exponent implies increasing deviation off the steady state. Thus, negative definiteness is the criterion for stability. We are going to apply this linear stability analysis together with numerical solutions of the coupled differential equations to determine the stability of the steady states.

## VI. SOLUTIONS OF THE DRIFT EQUATIONS

### A. Incoherent pumping

First, let us consider the simplest case when no atomic coherence is injected initially into the resonator, $|\rho_{ij}| = 0$, $i,j = a,b,c$. It follows that $R_k = 0$, $k = 1,2,3,4$ [see Eqs. (5.12)–(5.15)], and the equations of motion for the two phases reduce to simple forms. In particular, the relative phase satisfies the equation

$$\dot{\theta} = \frac{\alpha}{2N_1} (\rho_{bb} - \rho_{cc}) \sin(\phi - \theta). \tag{6.1}$$

The stable steady-state solutions of this equation are

$$\theta = \begin{cases} \phi & \text{if } \rho_{bb} > \rho_{cc} \\ \phi + \pi & \text{if } \rho_{bb} < \rho_{cc}, \end{cases} \tag{6.2}$$

while there is no stable solution for equal lower-level populations. The relative phase of the two modes is locked to a value that is essentially controlled by the phase of the external field. However, switching the sign of the initial inversion between the two lower levels will result in a $\pi$ jump in the steady-state relative phase. Since mode 1 drives the $|a\rangle \rightarrow |b\rangle$ transition and mode 2 the $|a\rangle \rightarrow |c\rangle$, the phase of the mode coupling the upper level to the dominantly populated lower level will be ahead of the other one. The intensities corresponding to the possible stable steady states read as

$$\tilde{I}_1 = \tilde{I}_2 = \begin{cases} \alpha(\rho_{aa} - \rho_{cc}) - 1 & \text{if } \rho_{bb} > \rho_{cc} \\ \alpha(\rho_{aa} - \rho_{bb}) - 1 & \text{if } \rho_{bb} < \rho_{cc}. \end{cases} \tag{6.3}$$

The intensities in the two modes are equal and determined by the inversion between the upper and the less populated lower level only. The population of the other lower level can be arbitrarily large, e.g., larger than that of the upper one (no inversion), without affecting the laser operation. It is "hidden" from the lasing mechanism and results in no extra absorption of the radiation. In particular, if one of the lower levels is empty laser operation can be achieved for arbitrarily small upper level population. This is clearly the effect of the external field coupling the lower two levels. The generated coherence between these two levels destructs the absorptive transition from the dominantly populated lower level to the upper one. The threshold of the laser is given by $\alpha_{\text{th}} = (\rho_{aa} - \rho_{xx})^{-1}$, where $\rho_{xx}$ is the population of the less populated lower level.

### B. Injected atomic coherence between the lower levels: $\rho_{bc}$

Since $\rho_{ab}$ and $\rho_{ac}$ are still assumed to be zero, $R_k = 0$, $k = 1,2,3,4$ [see Eqs. (5.12)–(5.15)] and the equation of motion for the relative phase is given by

$$\dot{\theta} = \frac{\alpha}{2N_1} [(\rho_{bb} - \rho_{cc}) \sin(\phi - \theta) + 2|\rho_{bc}| \sin(\varphi_{bc} + \phi)$$

$$\times \cos(\phi - \theta)]. \tag{6.4}$$

Assuming different lower-level populations, $\rho_{bb} \neq \rho_{cc}$, the stable solutions for the steady-state relative phase read the same as given above in Eq. (6.2), provided the initial phases of the injected coherence and the external field are set to $\varphi_{bc} + \phi = 0$ (or $\pi$) for $\rho_{bb} > \rho_{cc}$ (or $\rho_{bb} < \rho_{cc}$). However, due to the injected coherence a stable solution can also be found for the case of equal lower-level populations, $\rho_{bb} = \rho_{cc}$. The criterion for the particular value of the phase locking, in this case, is connected to the initial phase of the injected coherence and the external field, as given by

$$\theta = \begin{cases} \phi + \pi/2 & \text{if } \sin(\varphi_{bc} + \phi) < 0 \\ \phi - \pi/2 & \text{if } \sin(\varphi_{bc} + \phi) > 0, \end{cases} \qquad (6.5)$$

while the cases of $\phi - \varphi_{bc} = 0$ or $\pi$ are not stable. The corresponding steady-state intensities read as

$$\widetilde{I}_{1,2} = (\alpha \rho_{aa} - 1)\left[ 1 \pm \frac{2|\rho_{bc}|\cos(\varphi_{bc} + \phi)}{\rho_{bb} + \rho_{cc}} \right], \qquad (6.6)$$

where the upper (lower) sign corresponds to the first (second) mode. As we have seen above when finding the stable steady-state phases, in the case of different lower-level populations, $\rho_{bb} \neq \rho_{cc}$, $\cos(\varphi_{bc} + \phi)$ must be set to $\pm 1$, provided $\rho_{bb}$ is larger ($+1$) or smaller ($-1$) than $\rho_{cc}$. Looking at Eq. (6.6), the intensity of one of the modes can, in this case, be adjusted by controlling the amplitude of the injected coherence, $|\rho_{bc}|$, at the expense of the intensity of the other mode. Since $|\rho_{bc}| = \sqrt{\rho_{bb}\rho_{cc}}$ this can be done by adjusting the initial populations in the lower levels. On the other hand, for equal lower-level populations, $\rho_{bb} = \rho_{cc}$, the intensities are controlled by the phase of the injected coherence via varying $\cos(\varphi_{bc} + \phi)$. Consequently, the intensities in the two modes can be redistributed in both cases, when the lower-level populations are different or equal, by controlling the free parameter, amplitude, or phase of the injected coherence. In the most extreme cases one of the modes can be switched off completely, e.g., $\widetilde{I}_1 \cong 0$, making at the same time the intensity of the other mode increase to $\widetilde{I}_2 \cong 2(\alpha\rho_{aa} - 1)$. This is twice as large as the balanced intensities in the case of incoherent pumping in Sec. VI A, since all the energy is being concentrated in one of the modes only.

One should also note when comparing Eq. (6.6) to Eq. (6.3) that, in the present case, neither of the lower levels appears in the prefactor of the formula. Their populations do not affect the total intensity in the two modes, they merely allow for a continuous switching of the intensity from one mode to the other. That is, LWI appears naturally in the present case corresponding to the highest gain possible in the incoherently pumped system. The present scheme reproduces the incoherent one when one of the lower levels is empty or when $\cos(\varphi_{bc} + \phi)$ is zero. (Notice that it is not enough to set the coherence $|\rho_{bc}|$ to zero since we have already made use of the relation $|\rho_{bc}| = \sqrt{\rho_{bb}\rho_{cc}}$.)

### C. Injected atomic coherence between the upper and one of the lower levels: $\rho_{ab}$ or $\rho_{ac}$

Let us consider now injected coherence between the upper and one of the lower two levels, for example, $\rho_{ab}$. In the case when $\rho_{bb} < \rho_{cc}$ we found one solution, called regime
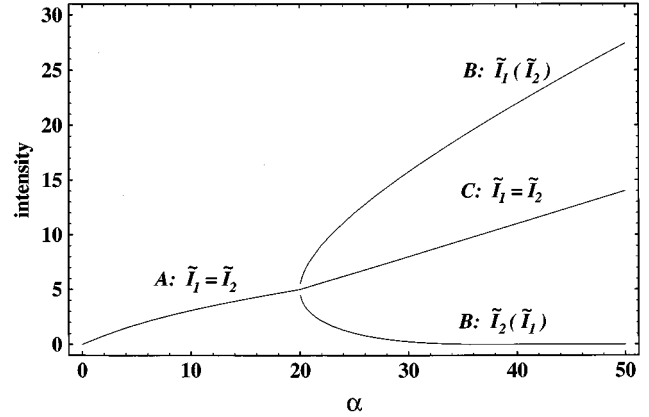


FIG. 2. Steady-state normalized intensities of the two modes $\widetilde{I}_1$ and $\widetilde{I}_2$ as functions of the pumping parameter $\alpha$. Atoms are injected in a coherent superposition of levels $a$ and $b$ the populations of which are $\rho_{aa} = 0.4$ and $\rho_{bb} = 0.5$. At a critical value of the pumping, $\alpha_{\text{crit}} = 20$, regime $A$ splits up into three new branches where, in regime $B$, the intensities of the two modes alternatively occupy the upper and lower branches in the figure (bistability) while in $C$ they stay equal.

$A$, that is stable for any pumping $\alpha$. The phases of the two modes, in this case, are locked to the phase of the injected coherence, $\theta_1 = \varphi_{ab} - \pi/2$ and $\theta_2 = \varphi_{ab} + \pi/2 - \phi$, resulting in the relative phase $\theta = \phi + \pi$. The intensities are equal, $\widetilde{I} \equiv \widetilde{I}_1 = \widetilde{I}_2$, determined by the equation

$$\widetilde{I}^{3/2} - [\alpha(\rho_{aa} - \rho_{bb}) - 1]\widetilde{I}^{1/2} - 2\alpha|\rho_{ab}| = 0. \qquad (6.7)$$

The injected atomic coherence provides a new driving term, viz., the third term on the left-hand side of the equation. One consequence is that, when solving Eq. (6.7), nonzero intensity can be found for any initial population of the three atomic levels including the most extreme cases where the population in the upper level is arbitrarily small. That is, the active atoms do not need to be inverted and LWI can be realized. On the other hand, laser action can be achieved at arbitrarily small pumping as illustrated by the example depicted in Fig. 2 due to the extra driving provided by the injected atomic coherence (radiating atomic dipole). Therefore we have stable operation without inversion and without threshold on the entire domain of $\alpha$.

Let us now look at the case when $\rho_{bb} > \rho_{cc}$. The system, in this case, exhibits three different stable regimes at steady state denoted by $A$, $B$, and $C$. An example is depicted in Fig. 2. We have already seen regime $A$ above. However, in the present case it is not stable for any pumping parameter but becomes unstable in the region of large $\alpha$ where regimes $B$ and $C$ take over (starting from $\alpha = 20$ in the figure). In particular, at the critical value of the pumping where regime $A$ becomes unstable the system has three different ways to go, i.e., becomes tristable. In regime $B$, the stable steady-state phases do not change as compared to regime $A$ but the intensities of the two modes separate according to

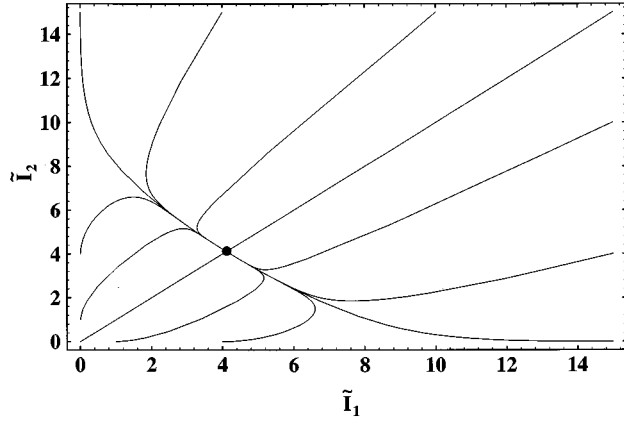$$\widetilde{I}_1^{1/2} = R \pm \sqrt{\alpha(\rho_{aa} - \rho_{cc}) - 1 - R^2}, \qquad (6.8)$$

FIG. 3. Evolution toward a single-valued steady state in regime $A$ at $\alpha = 15$ of Fig. 2 where $\phi = \varphi_{ab} = 0$ and the initial conditions for the phases are $\theta_{1,0} = -\theta_{2,0} = -\pi/2$ (i.e., starting from the steady-state value of the phases). The steady-state intensities are equal ($\widetilde{I}_1 = \widetilde{I}_2 \cong 4$) as indicated by a spot in the figure.

$$\widetilde{I}_2^{1/2} = R \pm \sqrt{\alpha(\rho_{aa} - \rho_{cc}) - 1 - R^2}, \qquad (6.9)$$

where $R \equiv 2|\rho_{ab}|/(\rho_{bb} - \rho_{cc})$. The switch from regime $A$ to $B$ occurs at the critical value of the pumping given by $\alpha_{\text{crit}} = (1 + R^2)/(\rho_{aa} - \rho_{cc})$. This critical point corresponds to the equal intensities, $\widetilde{I} = \widetilde{I}_1 = \widetilde{I}_2 = R^2$. The two alternative signs in Eqs. (6.8) and (6.9) suggest that regime $B$ provides a bistable operation where the intensities of the two modes can be interchanged: they can alternatively occupy the upper and lower branches in Fig. 2. We note that this scheme realizes a noninversion laser system where the intensities are determined by the inversion between the upper and the less populated lower level.

The third branch in Fig. 2 corresponds to regime $C$ and also starts from $\alpha_{\text{crit}}$. Here, the intensities of the two modes are equal, $\widetilde{I} \equiv \widetilde{I}_1 = \widetilde{I}_2$, and explicitly read as

$$\widetilde{I} = \alpha(\rho_{aa} - \rho_{cc}) - 1. \qquad (6.10)$$

This brings us back to the intensities found in the case of incoherent pumping given by Eq. (6.3). However, in the present case the phase locking between the two modes is different. It is a function of the intensity (i.e., the pumping parameter, $\alpha$) and, using Eq. (6.10), can be found from $\sin(\varphi_{ab} - \theta_1) = -\sin(\varphi_{ab} - \theta_2 - \phi) = R/\sqrt{\alpha(\rho_{aa} - \rho_{cc}) - 1}$. That is, injected coherence does not affect the intensities in regime $C$ but modifies the region of stability and the steady-state phases of the two modes.

In summary, the system exhibits critical behavior as a function of the pumping parameter $\alpha$. Regime $A$, occupying the region of low pumping rate, starts from zero threshold and realizes LWI. An example for the evolution of the intensities in the phase space, $\widetilde{I}_1 - \widetilde{I}_2$, toward, in this case, a single-valued steady state is depicted in Fig. 3. The time-dependent behavior of the field is obtained by numerically solving the system of differential equations for the intensities
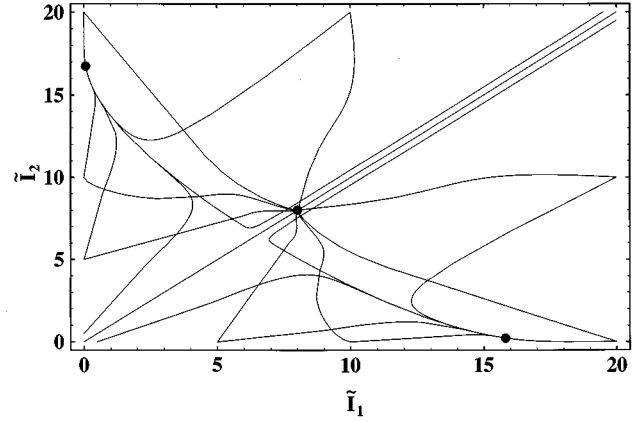


FIG. 4. Evolution toward a tristable steady state of regimes $B$ and $C$ at $\alpha = 30$ of Fig. 2 using $\phi = \varphi_{ab} = 0$. For the initial phases $\theta_{1,0} = \theta_{2,0} = 0$, the steady state corresponding to regime $C$ is realized (see spot in figure at $\widetilde{I}_1 = \widetilde{I}_2 = 8$). For $\theta_{1,0} = -\theta_{2,0} = -\pi/2$ we have two stable pairs of intensities where $\widetilde{I}_1$ and $\widetilde{I}_2$ are, respectively, equal to 0.25 and 15.8. They correspond to the two branches of regime $B$ in Fig. 2, and are realized depending on the initial conditions for the intensities.

and the phases given by the drift equations [see Eq. (5.19)]. The results confirm that regime $A$ is stable, remains stable for any pumping, and is the only stable operation when $\rho_{bb} < \rho_{cc}$. In the case when $\rho_{bb} > \rho_{cc}$, regime $A$ becomes unstable and splits into three new branches at a critical value of the pumping, $\alpha_{\text{crit}}$. These are regimes $B$ and $C$, all in noninversion operation. Regime $B$ itself is bistable while $C$ is single valued. Typical evolution toward the tristable steady state in the phase space, $\widetilde{I}_1 - \widetilde{I}_2$, is depicted in Fig. 4. The numerical solutions confirm the results obtained from the analytical stability analysis for the stable steady states. They also demonstrate that the time evolution toward steady state depends critically on the initial conditions. It can be seen in the figure that starting from the same intensities but different phases the system will evolve into a different steady state. Finally, we note that the system exhibits similar behavior with injected coherence $\rho_{ac}$, but with the roles of $\rho_{bb}$ and $\rho_{cc}$ interchanged.

### D. Injected atomic coherence between all the levels: $\rho_{ab}$, $\rho_{ac}$, and $\rho_{bc}$

We now consider the scheme where all the possible atomic coherences, $\rho_{ab}$, $\rho_{ac}$, and $\rho_{bc}$, are injected. It is found that stable steady-state operation can be achieved for arbitrary initial population of the atomic levels provided the phase of the external field is locked to the phase of the injected lower level coherence as $\varphi_{bc} + \phi = 0$ or $\pi$. Let us set, in particular, the initial population as $\rho_{bb} > \rho_{cc}$ and select the arbitrary phases to be $\varphi_{bc} + \phi = \pi$; the consequences of the other alternative settings will be discussed at the end of this subsection. In this parameter region, an example for the steady-state intensities of the two modes as functions of the pumping parameter $\alpha$ is given in Fig. 5 where the solid and dashed lines depict the intensities of the first and second
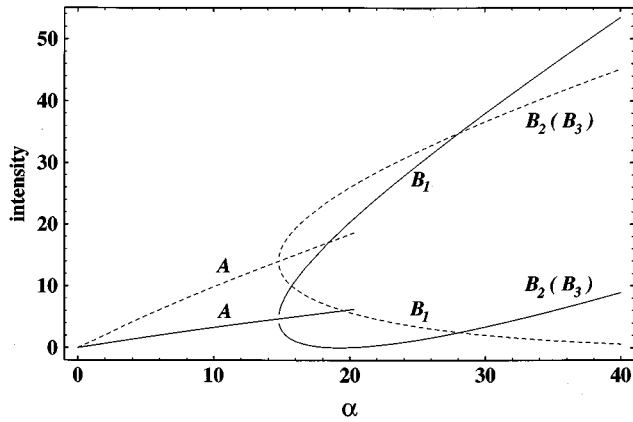
FIG. 5. Normalized steady-state intensities of the two modes $\widetilde{I}_1$ (solid line) and $\widetilde{I}_2$ (dashed line) vs pumping parameter $\alpha$ when all injected atomic coherences, $\rho_{ab}$, $\rho_{ac}$, and $\rho_{bc}$, are assumed. The initial population of the states are $\rho_{aa}=0.7$ and $\rho_{bb}=0.28$. Structures similar to Fig. 2 are apparent: regimes $A$ of each mode split up into two respective branches, $B_1$ and $B_2$ ($B_3$), at a critical point, $\alpha \cong 14.8$. The two equal-intensity regimes, $B_2$ and $B_3$, exhibit phase bistability.

modes, respectively. The curves are labeled with the letters $A$, $B_1$, $B_2$, and $B_3$, indicating the various regimes that we are going to consider in detail.

In regime $A$, the steady-state phases of the two modes are locked to the phases of the individual injected atomic coherences as $\theta_1 = \varphi_{ab} - \pi/2$ and $\theta_2 = \varphi_{ac} - \pi/2$. It follows from the relation $\varphi_{ab} + \varphi_{ac} = \varphi_{bc}$ that the relative phase between the modes locks to $\theta = -\varphi_{bc}$ that is equal to $\phi + \pi$ (see presumption in the previous paragraph). The corresponding intensities of the two modes are calculated from the equation given by

$$\widetilde{I}_2^{3/2} - \frac{M_2}{\rho_{bb}+\rho_{cc}} \{ \alpha[\rho_{aa}-(\rho_{bb}+\rho_{cc})]-1 \} \widetilde{I}_2^{1/2} - \frac{2\alpha R_2 M_2}{\rho_{bb}+\rho_{cc}}$$
$$= 0 \tag{6.11}$$

and

$$\widetilde{I}_1^{1/2} = \frac{R_1}{R_2} \widetilde{I}_2^{1/2}, \tag{6.12}$$

where $R_1$, $R_2$, and $M_2$ are defined by Eqs. (5.12), (5.13), and (5.9), respectively. From the stability analyses we find that this particular steady state in regime $A$ is stable for pumping parameters below the critical pumping $\alpha'_{\text{crit}}$, which reads as

$$\alpha'_{\text{crit}} = \frac{1 + 4\rho_{aa}(\rho_{bb}+\rho_{cc})/(\rho_{bb}-\rho_{cc})^2}{\rho_{aa}-2\rho_{cc}}. \tag{6.13}$$

We want to note that this critical point corresponds to an upper limit in the intensities given by $\widetilde{I}_2^{1/2} < 2\rho_{aa}/(\rho_{ab}-\rho_{ac})$. It follows from Eq. (6.11) that injected coherence

results in an extra driving term and, as depicted in Fig. 5, the threshold of the laser is zero. It can also be seen that the intensities are connected to the inversion between the upper and the two lower levels combined. Thus, none of the two lower levels is hidden in this scheme but, since solutions can be found for arbitrarily large lower-level populations, LWI is realized nevertheless. Equation (6.11) is a generalization of Eq. (6.7) in which scheme $\rho_{ab}$ is injected only. In fact, in the particular case of $\rho_{cc}=0$ Eqs. (6.11) and (6.12) reduce to Eq. (6.7) and the critical points of stability coincide exactly, as expected.

Next, let us look at the remaining three regimes, $B_1$, $B_2$, and $B_3$, together. The steady-state phases in regimes $B_1$ and $B_2$ are the same as in regime $A$ while in regime $B_3$ the phase of the first mode switches to $\theta_1 = \varphi_{ab} + \pi/2$ and the relative phase to $\theta = -\varphi_{bc} + \pi$. The intensities are given by the equations

$$\widetilde{I}_1^{1/2} = \frac{2}{\rho_{bb}+\rho_{cc}} \left[ R_1 \pm R_2 \left( \frac{\rho_{bb}+\rho_{cc}}{4\rho_{aa}} (\alpha\rho_{aa}-1)-1 \right)^{1/2} \right], \tag{6.14}$$

$$\widetilde{I}_2^{1/2} = \frac{2}{\rho_{bb}+\rho_{cc}} \left[ R_2 \pm R_1 \left( \frac{\rho_{bb}+\rho_{cc}}{4\rho_{aa}} (\alpha\rho_{aa}-1)-1 \right)^{1/2} \right], \tag{6.15}$$

where the upper signs correspond to regimes $B_1$ and $B_3$ and the lower ones to $B_2$. The stability analysis suggests that these regimes are all stable above a critical value of the pumping parameter given by

$$\alpha_{\text{crit}} = \frac{3\rho_{aa}+1}{\rho_{aa}(\rho_{bb}+\rho_{cc})}. \tag{6.16}$$

It follows from Eqs. (6.14) and (6.15) and from the steady-state phases above (see also Fig. 5) that regimes $B_2$ and $B_3$ exhibit phase bistability; the intensities in the two regimes are the same for any pumping but the phases (actually $\theta_1$ and $\theta$ only) have two different stable steady states. It can also be seen from the factor $(\alpha\rho_{aa}-1)$ that both lower levels are absent from the inversion term and, therefore, these regimes realize an optimum scheme for LWI where the population of the lower levels can be arbitrarily large. On the other hand, regimes $B_1$, $B_2$, and $B_3$ result in a splitting of the intensities of regime $A$ at the critical pumping $\alpha_{\text{crit}}$ (see Fig. 5) reminiscent of that in Sec. VI C. The present scheme is more complicated, however, because the intensities of the two modes in regime $A$ are not equal and, therefore, each branch splits up into two separate branches, $B_1$ and $B_2$ ($B_3$), individually. Nevertheless, the two systems correspond to one another both in their regimes $A$, as discussed above, and in their regimes $B$. Apart from regime $C$ missing from the present system, the two schemes exhibit similar dynamical behaviors approaching the same structure when $\rho_{cc}$ is decreasing. In particular, when $\rho_{cc}=0$ the two systems coincide exactly, as expected.

The scheme considered so far in the present subsection corresponds to the particular choice of $\rho_{bb} > \rho_{cc}$ and $\varphi_{bc} + \phi = \pi$. Let us briefly summarize what happens when selecting the other alternatives. Switching to $\varphi_{bc} + \phi = 0$ results in an exact interchange of the intensities, $\tilde{I}_1 \Leftrightarrow \tilde{I}_2$ (i.e., switch of the solid and dashed lines in Fig. 5), and in a shift of the phase of one of the modes, depending on the regime, by $\pi$ with respect to its steady-state value above. In particular, for $\rho_{bb} > \rho_{cc}$ $\theta_1$ switches in regimes $A$, $B_1$, and $B_2$ while $\theta_2$ switches in $B_3$. For $\rho_{bb} < \rho_{cc}$ it is reversed, $\theta_1$ shifts in $B_3$ and $\theta_2$ in $A$, $B_1$, and $B_2$. On the other hand, switching from $\rho_{bb} > \rho_{cc}$ to $\rho_{bb} < \rho_{cc}$ and keeping the value of $\varphi_{bc} + \phi$ the same results in an interchange of $\rho_{bb} \Leftrightarrow \rho_{cc}$ in the above formulas determining, for example, the magnitudes of the intensities or the locations of the critical points.

As a summary to this subsection, we can say that the system in this scheme operates in several different regimes in a multistable way exhibiting critical behavior. The intensities are single valued in the small pumping region starting from zero threshold while, at a critical point, they split up into tristable structures, reminiscent of those in Sec. VI C. The phases of the two modes lock to the phases of the injected coherences between the upper and lower levels as $\theta_1 = \varphi_{ab} \pm \pi/2$ and $\theta_2 = \varphi_{ac} \pm \pi/2$ depending on the initial parameters and the actual regime of operation. Above the critical point the system also exhibits phase bistability. This scheme realizes LWI in a crucially unstable way due to injected atomic coherences and the interplay between the two coexisting modes.

## VII. SUMMARY

We investigated the interaction of $\Lambda$-type three-level atomic systems with two modes of the radiation field where the lower two closely spaced levels of the atoms are coupled by an external field. In addition, we also assumed initial atomic coherences between various levels of the active atoms. The purpose of the present paper was to study multimode effects in LWI together with other quantum coherence phenomena due to injected atomic coherences. After solving the Schrödinger equation of the model in the interaction picture we calculated the master equation for the two-mode field-density matrix. The master equation was converted into a Fokker-Planck equation for the $P$ representation. From the drift coefficients we then obtained the coupled equations of motion for the average intensities and phases in the two modes. We solved these equations for various initial conditions and control parameters of the system such as the initial populations of the atoms, injected coherences, phase of the external field, etc.

We found that LWI in both modes is possible as a result of the external driving field. Similarly to the single-mode case [5], the coherence induced between the two lower levels results in nonabsorbing resonances between the upper and the lower levels of the atoms and, therefore, the population in one (or both) of the lower levels can be excluded from the consideration of the effective population inversion for lasing action. We also found that the relative phase of the two modes is locked to the phase of the external field. In addition, including injected atomic coherences into the system laser action can be realized with arbitrarily small pumping

rate (zero threshold) in both modes [5]. This is due to the injected atomic dipoles radiating independently of the actual gain-loss ratio in the system. In conclusion, we have shown that lasing without inversion can be achieved at zero-threshold operation in two phase-locked modes simultaneously.

We also found that injected atomic coherence between the lower two levels of the atoms can be used to redistribute the intensity between the two competing modes. In particular, one of the modes can be shut down, making the other mode two times ''brighter'' as compared to the symmetrical case. It can also be seen in this scheme that none of the lower-level populations appears in the inversion factor in the intensity formula; only that of the upper level appear. This suggests that both lower levels correspond to nonabsorbing resonances in this scheme. On the other hand, injecting atomic coherence between the upper and one of the lower levels of the system, besides zero-threshold LWI, gives rise to critical multimode behavior. We found multiple branching at critical points of the pumping parameter at steady state where the so far equal intensities can split into different branches. In particular, the intensities of the two modes can exhibit bistable and tristable behavior at steady state accompanied by single-valued phases in this scheme. These phenomena become more complicated when coherences between all atomic levels are injected. In this case, the intensities of the two modes are different for all pumping rates and, therefore, the multiple branching takes place on each mode's intensity separately. Besides intensity multistability, we found phase bistability in other regions of the pumping parameter where single-valued intensities are accompanied with phases having two stable steady states simultaneously.

This critical behavior suggests that the dynamics of the system can become essentially multistable and/or unstable and highly sensitive to initial conditions when more than one mode are present in the resonator. Therefore, in order to realize lasing without inversion in experiments in a stable way, mode selection is crucial. On the other hand, the system can also become a candidate for investigating critical phenomena where the goal actually would be to realize and study instabilities.

## ACKNOWLEDGMENTS

## APPENDIX

The Fokker-Planck equation given by Eq. (5.1) has been obtained from the master equation given implicitly by Eq. (4.3) according to the following standard procedure. Substituting the Glauber-Sudarshan $P$ representation of the field-density matrix,

$$\rho_F(t) = \int d^2\alpha_1 d^2\alpha_2 P(\alpha_1, \alpha_1^*, \alpha_2, \alpha_2^*, t) |\alpha_1, \alpha_2\rangle\langle\alpha_1, \alpha_2|,$$
(A1)

into the master equation, we obtain the equation of motion for $P(\alpha_1, \alpha_1^*, \alpha_2, \alpha_2^*, t)$,

$$\frac{1}{\gamma_c}\frac{\partial P}{\partial t} = \{-\partial_{\alpha_1}d_{\alpha_1} - \partial_{\alpha_1^*}d_{\alpha_1^*} + \partial^2_{\alpha_1\alpha_1}D_{\alpha_1\alpha_1} + \partial^2_{\alpha_1^*\alpha_1^*}D_{\alpha_1^*\alpha_1^*} + \partial^2_{\alpha_1\alpha_1^*}D_{\alpha_1\alpha_1^*} - \partial_{\alpha_2}d_{\alpha_2} - \partial_{\alpha_2^*}d_{\alpha_2^*} + \partial^2_{\alpha_2\alpha_2}D_{\alpha_2\alpha_2} + \partial^2_{\alpha_2^*\alpha_2^*}D_{\alpha_2^*\alpha_2^*}$$

$$+\partial^2_{\alpha_2\alpha_2^*}D_{\alpha_2\alpha_2^*} + \partial^2_{\alpha_1\alpha_2}D_{\alpha_1\alpha_2} + \partial^2_{\alpha_1^*\alpha_2^*}D_{\alpha_1^*\alpha_2^*} + \partial^2_{\alpha_1\alpha_2^*}D_{\alpha_1\alpha_2^*} + \partial^2_{\alpha_1^*\alpha_2}D_{\alpha_1^*\alpha_2}\}P + \cdots , \tag{A2}$$

where $P = P(\alpha_1, \alpha_1^*, \alpha_2, \alpha_2^*, t)$. Here, we used the notation $\partial_{\alpha_i} = \partial/\partial\alpha_i$ and $\partial^2_{\alpha_i\alpha_j} = \partial^2/\partial\alpha_i\partial\alpha_j$ for the derivatives while the higher-order terms, $\partial^3_{\alpha_i\alpha_j\alpha_k}$, $i,j,k = 1,2$, are omitted. Instead of dealing with this form of the Fokker-Planck equation we transform it into polar form, where $P$ is now considered as a function of the intensities $I_1$, $I_2$ and phases $\theta_1, \theta_2$ of the two modes. These are defined by the substitutions $\alpha_1 \equiv \sqrt{I_1}e^{i\theta_1}$ and $\alpha_2 \equiv \sqrt{I_2}e^{i\theta_2}$. After introducing the normalized intensities, $\tilde{I}_1$ and $\tilde{I}_2$, defined in Sec. V, the Fokker-Planck equation given by Eq. (A2) becomes Eq. (5.3). The drift terms in this equation are given in Sec. V, while here we present the diffusion coefficients assuming that $\langle I_1 \rangle$ and $\langle I_2 \rangle \gg 1$ still holds. Then the diffusion terms are given by

$$D_{\tilde{I}_1\tilde{I}_1} = \frac{\beta\tilde{I}_1}{(N_1N_2)^2}\left\{\rho_{aa}\left(1 + \frac{1}{2}\tilde{I}_2\right)N_1^2 + \frac{1}{16}\bar{M}_1\tilde{I}_1N_2^2 + \frac{3}{16}(\bar{M}_1\tilde{I}_1 + \bar{M}_2\tilde{I}_2)\left[N_1N_2 - \frac{\tilde{I}_1}{8}(2N_2+3)\right]\right\}, \tag{A3}$$

$$D_{\tilde{I}_1\tilde{I}_2} = -\frac{\beta\tilde{I}_1\tilde{I}_2}{(N_1N_2)^2}\left\{\rho_{aa}N_1^2 + \frac{1}{16}(\bar{M}_1+\bar{M}_2)N_2^2 + \frac{3}{64}(\bar{M}_1\tilde{I}_1 + \bar{M}_2\tilde{I}_2)(N_1N_2+3)\right\}, \tag{A4}$$

$$D_{\theta_1\theta_1} = \frac{\beta}{4\tilde{I}_1N_1^2N_2}\left\{\rho_{aa}\left(1 + \frac{1}{4}\tilde{I}_1\right)N_1^2 - \frac{1}{16}\bar{M}_1\tilde{I}_1N_2 + \frac{3}{16}(\bar{M}_1\tilde{I}_1 + \bar{M}_2\tilde{I}_2)\left[N_1 + \frac{\tilde{I}_1}{24}(2N_1+3)\right]\right\}, \tag{A5}$$

$$D_{\theta_1\theta_2} = \frac{\beta}{8N_1^2N_2}\left\{\rho_{aa}N_1^2 - \frac{1}{8}(\bar{M}_1+\bar{M}_2)N_2 + \frac{1}{32}(\bar{M}_1\tilde{I}_1 + \bar{M}_2\tilde{I}_2)(2N_1+3)\right\}, \tag{A6}$$

$$D_{\tilde{I}_1\theta_1} = \frac{\beta\sqrt{\tilde{I}_1/\tilde{I}_2}}{32N_1^2N_2}\left\{\tilde{I}_1\tilde{I}_2\left(\frac{R_3}{\sqrt{\tilde{I}_2}} - \frac{R_4}{\sqrt{\tilde{I}_1}}\right)(N_1-3) - 2\tilde{I}_2\left(M_b - 4\frac{R_3}{\sqrt{\tilde{I}_2}}\right)N_2\right\}, \tag{A7}$$

$$D_{\tilde{I}_1\theta_2} = \frac{\beta\sqrt{\tilde{I}_1/\tilde{I}_2}}{32N_1^2N_2}\left\{\tilde{I}_1\tilde{I}_2\left(\frac{R_3}{\sqrt{\tilde{I}_2}} - \frac{R_4}{\sqrt{\tilde{I}_1}}\right)(N_1-3) - \tilde{I}_2\left(M_b - 4\frac{R_3}{\sqrt{\tilde{I}_2}}\right)N_2 + \tilde{I}_1\left(M_b - 4\frac{R_4}{\sqrt{\tilde{I}_1}}\right)N_2\right\}, \tag{A8}$$

together with

$$D_{\tilde{I}_2\tilde{I}_2} = D_{\tilde{I}_1\tilde{I}_1}(\text{interchange}, \tilde{I}_1 \Leftrightarrow \tilde{I}_2 \text{ and } \bar{M}_1 \Leftrightarrow \bar{M}_2), \tag{A9}$$

$$D_{\theta_2\theta_2} = D_{\theta_1\theta_1}(\text{interchange}, \tilde{I}_1 \Leftrightarrow \tilde{I}_2 \text{ and } \bar{M}_1 \Leftrightarrow \bar{M}_2), \tag{A10}$$

$$D_{\tilde{I}_2\theta_2} = -D_{\tilde{I}_1\theta_1}(\text{interchange}, \tilde{I}_1 \Leftrightarrow \tilde{I}_2 \text{ and } R_3 \Leftrightarrow R_4), \tag{A11}$$

$$D_{\tilde{I}_2\theta_1} = -D_{\tilde{I}_1\theta_2}(\text{interchange}, \tilde{I}_1 \Leftrightarrow \tilde{I}_2 \text{ and } R_3 \Leftrightarrow R_4). \tag{A12}$$

Finally, we want to remark that the drift terms of the sum and difference phases, $\mu \equiv \theta_1 + \theta_2$ and $\theta \equiv \theta_1 - \theta_2$, and the sum and difference intensities, $\tilde{I}_\pm = \tilde{I}_1 \pm \tilde{I}_2$, can be calculated as the sums and the differences of the corresponding drift terms for the two modes. On the other hand, the corresponding diffusion coefficients read as

$$D_{\mu\mu} = D_{\theta_1\theta_1} + D_{\theta_2\theta_2} + D_{\theta_1\theta_2}, \tag{A13}$$

$$D_{\theta\theta} = D_{\theta_1\theta_1} + D_{\theta_2\theta_2} - D_{\theta_1\theta_2}, \tag{A14}$$

and

$$D_{\tilde{I}_\pm\tilde{I}_\pm} = D_{\tilde{I}_1\tilde{I}_1} + D_{\tilde{I}_2\tilde{I}_2} \pm D_{\tilde{I}_1\tilde{I}_2}, \tag{A15}$$

indicating that the noise in these quantities is connected to the cross correlations between the two modes. The cross terms of the sum-difference quantities are given by

$$D_{\mu\theta} = 2(D_{\theta_1\theta_1} - D_{\theta_2\theta_2}), \tag{A16}$$

$$D_{\tilde{I}_+\tilde{I}_-} = 2(D_{\tilde{I}_1\tilde{I}_1} - D_{\tilde{I}_2\tilde{I}_2}). \tag{A17}$$

[1] M. O. Scully, S.-Y. Zhu, and A. Gavrielides, Phys. Rev. Lett. **62**, 2813 (1989); about the $\Lambda$ system in general, see also O. Kocharovskaya and Ya. I. Khanin, Pis'ma Zh. Eksp. Teor. Fiz. **48**, 581 (1988) [JETP Lett. **48**, 630 (1988)]; O. Kocharovskaya and P. Mandel, Phys. Rev. A **42**, 523 (1990); E. E. Fill, M. O. Scully, and S.-Y. Zhu, Opt. Commun. **77**, 36 (1990).

[2] S. E. Harris, Phys. Rev. Lett. **62**, 1033 (1989); S. E. Harris and J. J. Macklin, Phys. Rev. A **40**, 4135 (1989); A. Imamoglu and S. E. Harris, Opt. Lett. **14**, 1344 (1989); A. Imamoglu, Phys. Rev. A **40**, 2835 (1989); A. Imamoglu, J. E. Field, and S. E. Harris, Phys. Rev. Lett. **66**, 1154 (1991); P. Mandel and O. Kocharovskaya, Phys. Rev. A **46**, 2700 (1992).

[3] L. M. Narducci, H. M. Doss, P. Ru, M. O. Scully, S.-Y. Zhu, and C. Keitel, Opt. Commun. **81**, 379 (1991); M. O. Scully, S.-Y. Zhu, L. M. Narducci, and H. Fearn, *ibid.* **81**, 240 (1992); S. Basile and P. Lambropoulos, *ibid.* **78**, 163 (1990); P. Mandel and O. Kocharovskaya, Phys. Rev. A **47**, 5003 (1993). For a review see, O. Kocharovskaya, Phys. Rep. **219**, 175 (1992); M. O. Scully, *ibid.* **219**, 191 (1991); P. Mandel, Contemp. Phys. **34**, 235 (1994), and references therein.

[4] G. Alzetta, A. Gozzini, L. Moi, and G. Orriols, Nuovo Cimento B **36**, 5 (1976); G. Alzetta, L. Moi, and G. Orriols, *ibid.* **52**, 209 (1979).

[5] J. A. Bergou and P. Bogár, Phys. Rev. A **43**, 4889 (1991); this is the single-mode version of the system discussed in the present paper.

[6] G. S. Agarwal, Phys. Rev. Lett. **67**, 980 (1991); K. Gheri and D. F. Walls, *ibid.* **68**, 3428 (1992); Phys. Rev. A **45**, 6675 (1992); Y. Zhu, *ibid.* **47**, 495 (1993); Y. Zhu, O. C. Mullins, and M. Xiao, *ibid.* **47**, 602 (1993).

[7] M. O. Scully, Phys. Rev. Lett. **55**, 2802 (1985); M. O. Scully, K. Wódkiewicz, M. S. Zubairy, J. Bergou, N. Lu, and J. Meyer ter Vehn, *ibid.* **60**, 1832 (1988); N. Lu and J. Bergou, Phys. Rev. A **40**, 237 (1989); J. Bergou, J. Zhang, and A. Hourri, *ibid.* **50**, 4188 (1994); N. Lu and S.-Y. Zhu, *ibid.* **40**, 5735 (1989).

[8] M. O. Scully, Phys. Rev. Lett. **67**, 1855 (1991); M. O. Scully and S.-Y. Zhu, Opt. Commun. **87**, 134 (1992); M. Fleischhauer, C. H. Keitel, M. O. Scully, C. Su, B. T. Ulrich, and S.-Y. Zhu, Phys. Rev. A **46**, 1468 (1992); A. D. Wilson-Gordon and H. Friedmann, Opt. Commun. **94**, 238 (1992); U. Rathe, M. Fleischhauer, S.-Y. Zhu, T. W. Hänsch, and M. O. Scully, Phys. Rev. A **47**, 4994 (1992); M. O. Scully, Phys. Rev. Lett. **69**, 1360 (1992).

[9] K.-J. Boller, A. Imamoglu, and S. E. Harris, Phys. Rev. Lett. **66**, 2593 (1991); J. E. Field, K. H. Hahn, and S. E. Harris, *ibid.* **67**, 3062 (1991); S. E. Harris, J. E. Field, and A. Kassapi, Phys. Rev. A **46**, R29 (1992); S. E. Harris, Phys. Rev. Lett. **70**, 552 (1993); **72**, 52 (1994); J. H. Eberly, M. L. Pons, and H. R. Hag, *ibid.* **72**, 56 (1994); A. Kassapi, Maneesh Jain, G. Y. Yin, and S. E. Harris, *ibid.* **74**, 2447 (1995).

[10] O. Kocharovskaya, P. Mandel, and M. O. Scully, Phys. Rev. Lett. **74**, 2451 (1995).

[11] S.-Y. Zhu, M. O. Scully, H. Fearn, and L. M. Narducci, Z. Phys. D **22**, 483 (1992).

[12] S.-Y. Zhu and M. O. Scully, Phys. Rev. Lett. **76**, 388 (1996); H. R. Xia, C. Y. Ye, and S.-Y. Zhu, *ibid.* **77**, 1032 (1996).